FORECASTING THE SPEED AND MAINTENANCE OF QUASI-LINEAR MESOSCALE CONVECTIVE SYSTEMS

Michael C. Coniglio

Harold E. Brooks

NOAA/OAR National Severe Storms Laboratory, Norman, OK

Steven J. Weiss

Stephen F. Corfidi

NOAA/Storm Prediction Center, Norman, OK

Manuscript submitted to

Weather and Forecasting

30 December 2005

Corresponding author address: Dr. Michael C. Coniglio
National Severe Storms Laboratory
1313 Halley Circle
Norman, OK 73069

ABSTRACT

The problem of forecasting the speed and maintenance of quasi-linear mesoscale convective systems (MCSs) is investigated through an examination of observed proximity soundings. Environmental variables that are statistically different between MCSs of different speeds and between mature and weakening MCSs are input into a logistic regression procedure to develop probabilistic guidance on MCS speed and maintenance. This study focuses on quasi-linear systems that persist for several hours.

Between the mature and weakening MCSs, shear vector magnitudes over very deep layers are the best discriminators among hundreds of kinematic and thermodynamic variables. The lapse rates over a significant portion of the convective cloud layer, the RUC convective available potential energy, and the deep-layer mean wind speed are also very good discriminators. Between the slow and fast forward-propagating systems, the deep-layer mean wind speed, and normalized values of the maximum vertical difference in equivalent potential temperature (θ_e) and low-to-mid-level lapse rates are the best discriminators.

Probabilistic equations developed from these variables used with short-term numerical model output are encouraging. The equations show utility in forecasting the transition of an MCS with a solid line of 50+ dbZ echoes to a more disorganized system with unsteady changes in structure and propagation. The equations may also provide guidance on the potential for an MCS to produce severe surface winds on regional scales. This study shows that empirical forecast tools based on environmental relationships still have the potential to provide forecasters with improved information on the qualitative characteristics of MCS speed, structure, and longevity. This is especially important since the current and near-term value added by explicit numerical forecasts of convection is still uncertain.

1. INTRODUCTION

Forecasting the details of mesoscale convective systems (MCSs) (Zipser 1982) continues to be a difficult problem. Recent advances in numerical weather prediction models and computing power have allowed for explicit real-time prediction of MCSs over the past few years (Davis et al. 2004, Kain et al. 2005). While these forecasts are promising, their utility and how to best use their capabilities in support of operations is unclear (Kain et al. 2005). Therefore, refining our knowledge of the interactions of MCSs with their environment remains central to advancing our near-term ability to forecast MCSs.

a. MCS speed

The speed of an MCS plays a significant role in both the likelihood of producing damaging surface winds and its longevity, but accurate estimates of MCS motion prior to MCS initiation are difficult at best. It is well known that the speed of a storm-induced cold pool strongly controls the overall MCS speed and can be estimated through the theoretical properties of density currents (Seitter 1986, Bryan et al. 2005). However, the observations required to make these calculations accurately aren't routinely available. Even if real-time calculations of this type were possible, predicting MCS speed is inherently nonlinear because it requires anticipating how the environment and system will interact to affect the advection and propagation of the system itself. This often leads to significant temporal and spatial variability of speeds associated with the leading line motion.

It is useful to consider the motion of the mean MCS centroid as the sum of the advection of cells by the mean flow and the propagation of the system as the result of new cell development (Chappell 1986). Useful estimates of the advective component can be provided by the mean cloud-layer wind (Corfidi 2003, Cohen et al. 2006). But forecasting MCS propagation is more

problematic since the cold pool of air that results from the evaporation/melting of precipitation always interacts with the environment. The ensuing regions of convergence along the cold pool and subsequent convective redevelopment can greatly influence the propagation of the parent MCS. Forecasting tools based on these principles have shown some skill in predicting the MCS direction of motion (Corfidi 2003), but anticipation of the near-term propagation characteristics (upwind versus downwind) and resultant speed of the MCS remains very difficult. This leads us to investigate more probabilistic methods to predicting the speed of MCSs.

b. MCS maintenance

Predicting MCS maintenance is fraught with challenges such as understanding how deep convection is sustained through system/environment interactions (Weisman and Rotunno 2004, Coniglio et al. 2005), how pre-existing mesoscale features influence the systems (Fritsch and Forbes 2001, Trier and Davis 2005), and how the system itself can alter the inflow environment and feed back to changes in the system structure and longevity (Parker and Johnson 2004c, Fovell et al. 2005).

Evans and Doswell (2001) provide observational evidence that the strength of the mean wind (0-6 km) and its effects on cold pool development and MCS motion play a significant role in sustaining long-lived forward-propagating MCSs that produce damaging surface winds (derechos) through modifying the inflow of unstable air. They also show that a wide range of convective available potential energy (CAPE) and vertical wind shear is found in the environments of derechos, likely reflecting the variety of forcing mechanisms present in the spectrum of cases.

Through the use of wind profiler observations and numerical model output, Gale et al. (2002) examine nocturnal MCSs to determine predictors of their dissipation. Similar to Evans and

Doswell (2001), they find that changes in MCS speed may control its dissipation through changes in low-level storm-relative inflow. However, despite some indications that a decreasing low-level-jet intensity and low-level equivalent potential temperature (θ_e), and its advection, can be useful in some cases, they did not find robust predictors of MCS dissipation.

The analysis of proximity soundings in Coniglio et al. (2004) also shows that CAPE and low-level wind shear varies considerably in derecho environments and that significant wind shear often exists in mid and upper levels in the pre-convective environment. An emphasis of this work is that wind shear over deeper layers than those considered in past idealized modeling studies (Weisman and Rotunno 2004) may be important for the maintenance of these systems. Stensrud et al. (2005) echoes this result and suggests this is especially true when the cold pool is very strong. This point may be particularly important because observations from the BAMEX[1] field campaign suggest that cold pools often extend to 3 to 5 km above ground (Bryan et al. 2005), which is deeper than cold pools in idealized simulations of convective systems (Coniglio and Stensrud 2001, Weisman and Rotunno 2004).

c. Goals

The first goal of this work is to briefly summarize some recent ideas on the importance of cold pool/deep shear environment interactions on MCS maintenance, which is presented in section 2. The second and primary goal of this work is to examine a large data set of observed proximity soundings to identify predictors of MCS speed and dissipation and to improve our understanding of MCS environments. The ultimate goal is to develop forecast tools that provide probabilistic guidance on the speed and maintenance of MCSs. The focus is on the 3-12 hour

[1] BAMEX stands for the Bow Echoes and Mesoscale Convective Vortex (MCV) Experiment, which was a field program designed to obtain high-density kinematic and thermodynamic observations in and around bow-echo MCSs and mesoscale convective vorticies (Davis et al. 2004).

time scale, which could benefit Day 1 Severe Weather Outlooks, Mesoscale Discussions, and the issuance of Severe Weather Watches at the Storm Prediction Center (SPC), and short-term forecasts issued by local National Weather Service forecast offices.

The approach taken in this study is to use statistical techniques on the predictors (described in section 3) to develop equations for the conditional probability of a strong, mature MCS and the probability of an MCS reaching a particular speed. This study focuses on the robust systems that obtain a quasi-linear leading line and tend to produce severe weather and strong cold pools, and therefore, we intend for this discussion to be most applicable to systems that are not strongly tied to frontal-scale forcing (Fritsch and Forbes 2001) or strong low-level jets (Trier and Parsons 2005). The "best" predictors of MCS speed and dissipation, the development of the probability equations, and some examples of their application are discussed in section 4. A final summary and discussion is given in section 5.

2. COLD POOL/SHEAR INTERACTIONS

For years, researchers have employed idealized convection-resolving numerical models to understand the physical importance of the environmental vertical wind shear (usually the low-level shear) in countering the effects of the cold pool and controlling the behavior of quasi-linear MCSs (see Weisman and Rotunno 2004 for a review). Weisman and Rotunno (2004) revisit many years of idealized modeling studies to show that quasi-linear MCS behavior is most sensitive to changes in the strength of the low-level shear, and that for stronger shears, deeper lifting and stronger systems are obtained if the shear is confined to low-levels.

Other researchers have looked at the effects of deeper shear on MCSs in more detail. In a set of idealized two-dimensional (2-D) simulations of squall lines, Fovell and Daily (1995) examine the effects of shear-layer depth for a fairly low to moderate value of vertical shear fixed

at 3 x 10^{-3} s^{-1}. As the shear-layer depth is increased, the model storms become stronger with more upright convective updrafts and longer periods of organized oscillatory behavior despite a decreasing amount of shear over a given low-level layer.

Similar squall line behavior is noted in Parker and Johnson (2004c), who examine the structures and dynamics of quasi-linear systems with 2-D and periodic 3-D simulations. They focus on the effects of vertical shear added above a fixed value of shear below 3 km. In the deep shear environments, convective updrafts interact with the positive shear to generate pressure perturbations that accelerate the flow downshear in mid and upper levels (this concept is illustrated in Fig. 1). These transient pressure perturbations account for a significant portion of the net overturning over time. As in some analytical studies of 2-D convection (Shapiro 1992, Moncrieff and Liu 1999), they hypothesize that the deeper shear gives parcels more upright trajectories and allows them to spend more time in the zone of upward accelerations.

This model of deep convective overturning in deep shear is examined further in Coniglio et al. (2005) through idealized 3-D numerical simulations of convective systems in varying amounts of vertical shear in the 5-10 km layer above a fixed amount of low-level shear (20 m s^{-1}/ 0-5 km). They show quantitatively that the addition of shear in the 5-10 km layer above the storm-induced cold pool can allow for much deeper lifting of the overturning air parcels and a much greater percentage of parcels that are lifted to higher levels (Fig. 2). They argue that the deeper shear predisposes the environment to placing a steering level (the level at which the cold pool speed matches the line-normal environmental wind speed) somewhere in mid and upper-levels. This allows the favorable downshear accelerations shown in Fig. 1 to keep the convective regions close to the cold pool leading edge, which facilitates the maintenance of the system as a whole. An emphasis of this work is that elevated parcels (above 1 km) are responsible for the

deep overturning in these deeper shear regimes. For a low-level shear of 20 m s^{-1}/0-5 km, the lifting is maximized for moderate upper-level shear values (10–15 m s^{-1}/5-10 km) (Fig. 2) and is manifest in quasi-2-D regimes as larger, stronger, more upright collections of line segments and bow echoes that persist for longer periods along the leading edge of the cold pool.

Parker and Johnson (2004a) provide a summary of observations of systems in which the mid to upper level shear may have been important to their maintenance. A recent example of one such case is the 9-10 June 2003 nocturnal bow echo-MCS event observed during BAMEX. The flow structure revealed by high-quality multiple Doppler analysis suggests that the parcels originating above 2 km (MSL) are overturning deeply and the parcels below this level are passing through the cold pool region (Fig. 3), similar to the conceptual model shown in Fig. 1 and in Coniglio et al. (2005). A special sounding taken in the inflow environment (Fig. 4) shows a complex low-level shear profile and a relatively dry surface layer that suggests a decoupling of the more stable surface air from the high θ_e air at 850 hPa and above. It is intriguing that the 700 – 300 h Pa layer has about 15-20 m s^{-1} of mean line-perpendicular shear (Fig. 4), which suggests that the enhancement in lifting from shear above the cold pool may have been important for this event, especially if the deep convective updrafts were rooted in the 850 – 750 hPa layer.

These recent studies suggest that physical mechanisms related to upper-level shear are relevant to both quasi 2-D and 3-D regimes of MCSs and that the low-level shear/cold pool interactions that can help to determine the strength and structure of the systems initially (Weisman and Rotunno 2004) do not provide a complete picture of the complex question of MCS structure and maintenance. This may be especially true once a strong, organized cold pool and deep mesoscale updrafts become established above a surface stable layer. This leads us to examine the observed environments of a large spectrum of MCSs, especially the shear profiles,

with a more discerning outlook if we are to develop a clearer understanding of their maintenance and propagation, and if we are to improve the methods for their prediction.

3. DEVELOPMENT OF FORECAST TOOLS

a. MCS proximity sounding data set

To develop a large data set of MCS proximity soundings, MCSs are identified by examining composites of base radar reflectivity for the months of May-August during the seven-year period of 1998-2004. We follow the Parker and Johnson (2000) description of MCSs and focus our attention on the type that have a nearly contiguous quasi-linear or bowed leading edge of reflectivity values of at least 35 dbZ at least 100 km in length. Although a 100 km-long collection of cells could be considered an MCS if it persists for 2-3 hours (Cotton et al. 1989), we only consider events that maintained this spatial configuration for at least 5 continuous hours to focus on the longer-lived events.

From a set of over 600 MCSs of this type, we identify 269 events in which a radiosonde observation was taken within about 200 km and 3 h of the leading edge of the MCS and displayed no obvious signs of contamination from convection. In addition, only those soundings that appeared to be in the inflow environment are included in this tally. We add 79 derecho proximity soundings that were identified using a similar procedure in Coniglio et al. (2004) to amass a set of 348 warm-season (May-August) MCS proximity soundings[2] (Fig. 5).

At the time of the proximity sounding, the appearance and trends of the radar reflectivity are used to assess the mean speed and direction of the leading-line MCS motion and the stage of the

[2] This data set is much more heavily weighted to high Plains events than the derecho-only data set of Evans and Doswell (2001) (c.f. Fig. 5 and their Fig. 3). For example, 25% (86 out of 348) of our soundings are in the central and northern Plains region west of the Missouri River, whereas only 5 % (6 out of 113) of Evans and Doswell's soundings are found in this region. This disparity in the geographical distribution of the soundings should be noted if one attempts to compare and interpret the results of both studies.

MCS in its life cycle. The motion is defined by averaging the motions observed along the line at several points at a given time, then averaging these values in a 3 hour window centered at the time of the sounding. Within this 3-hour window, the stage of the MCS in its lifecycle is defined as one of three stages: (1) initial cells prior to MCS development ("initiation"), (2) a mature MCS, with strengthening or quasi-steady high reflectivity (50 dBZ or higher) embedded within the nearly contiguous line of 35+ dbZ echoes ("mature"), and (3) a weakening MCS, with significantly weakened or shrinking areas of high reflectivity or a loss of system organization and associated areas of high reflectivity ("dissipation").

The predictors for MCS maintenance are identified from a subset of MCSs in which the leading line was moving ≥ 10 m s^{-1} near the sounding time. Although MCSs that move at speeds less than 10 m s^{-1} aren't necessarily physically distinct from faster moving systems, this helps to ensure that we are including systems with some cold pool propagation characteristics. This produces a subset of 290 soundings that are used in the identification of the MCS maintenance predictors. These soundings are then stratified into 79 "initiation," 96 "mature," and 115 "dissipation," soundings based on the appearance and trends of the radar reflectivity at the time of the sounding as described above.

To derive predictors for the speed of MCSs, we reinsert the soundings for which the line speed was < 10 m s^{-1} and remove the 120 dissipation soundings (5 of these are associated with line speeds < 10 m s^{-1} and are not included in the previous stratification). This focuses on the environmental conditions associated with the organizing and mature stages of the MCSs in the determination of the speed predictors. We stratify the remaining 228 soundings into two groups; the 130 soundings associated with MCS speeds (C) < 18 m s^{-1} and the 98 soundings associated with C ≥ 18 m s^{-1}. We choose a speed of 18 m s^{-1} as the break point because operational

experience suggests that systems moving faster than this speed have an increased likelihood of producing widespread damaging wind gusts (as long as the storms are rooted in the boundary layer), which is supported by the results in Cohen et al. (2006).

b. Statistical methods

Several hundred variables are calculated from the soundings that represent various aspects of the kinematic and thermodynamic environment. We focus on a subset of variables that are found to have the largest statistically significant differences among the MCS categories ("best discriminators") and focus on those variables that are emphasized in previous studies. The statistical procedure to identify the best discriminators and the development of the forecast tools are described next [we refer the reader to Wilks (1995) for details on the components of the procedure].

To assess the statistical differences, we use the Mann-Whitney test to identify variables that give the lowest probabilities (largest Z-scores) that the population "locations" (non-parametric analog to the mean) among the two groups in question are the same. Nonparametric tests like the Mann-Whitney test are attractive in applications with relatively small data sets since there is no requirement to assume an underlying distribution to the data sample, which is required in the widely used Student's t-test. We do not restrict our investigation to a handful of variables over a few layers but rather take a "brute force" approach by calculating various mean wind and wind shear over all possible layers ≥ 1 km deep up to 12 km. Several versions of CAPE and instability measures that require vertical differentiation (lapse rates, $\Delta\theta_e$) also are calculated over multiple layers. We then use the absolute magnitude of the Z-scores to compare each variable between the mature and dissipation soundings to identify the particular kinematic and instability variables that are the most different between the two groups.

Using the Z-scores as a guide, linear discriminant analyses are then used to find the number and particular combination of variables that provide the "best" separation among the two groups in question. This amounts to determining the combination of variables that produce the highest percentage of correctly-grouped soundings in a discriminant analysis. We find that the percentage of correct groupings converges to within 1-2% after the inclusion of only 3 to 4 variables in the analyses, which is a reflection of the substantial mutual correlations among the variables.

Once the variables that best discriminate between the two groups in question are identified, logistic regression[3] is used to develop an equation that gives the probability of one of the two groups occurring. Logistic regression is a method of producing probability forecasts on a set of binary data (or data within two groups) by fitting predictors to the equation

$$y = \frac{1}{1 + \exp[b_0 + b_1 x_1 + b_2 x_2 + \cdots + b_k x_k]} \qquad (1)$$

where y is the fractional probability of one of the groups occurring, k is the number of predictors, x_k refers to the kth predictor, and b_k refers to the kth regression coefficient for each predictor. Logistic regression is attractive in this context because the predictand is a probability, i.e., it allows for the direct computation of probabilities between two possible outcomes in a set of data.

c. Interpretation of the probability equations

The first part of section 4 focuses on forecasting the probability of MCS maintenance, which in this application amounts to finding the best discriminators between the 96 mature and 115 dissipation soundings. The logistic regression equation is thus designed to give the probability of a "mature" MCS as defined above, conditional on the development of an MCS. However, a

[3] We used the *Splus* version 6.1 software to perform logistic regression.

consequence of the experimental design is that the predicted intensity of the MCS is not independent of the predicted stage of the MCS. This is because many of the same variables that discriminate well between the mature and weakening stages of a particular MCS also appear to discriminate well between MCSs of different intensities (Cohen et al. 2006). For example, large versus small CAPE could mean a mature versus a weakening MCS *and* a strong versus weak MCS. Therefore, the higher the probability of MCS maintenance, the more likely it is that an MCS will be maintained *and* be strong in a given environment, but the relative contribution to MCS maintenance compared to MCS intensity can not be determined in a particular case.

The same ambiguity in interpretation of the probabilities applies to the MCS speed probabilities. The logistic regression equation in this case is designed so that predictors that result in y = 0.9 indicates that the MCS has a 90% chance of having a forward-propagating leading edge that moves at speeds ≥ 18 m s^{-1}. But the factors that lead to a fast-forward propagating cold pool also are related to the factors that produce strong systems (Cohen et al. 2006). We believe that this ambiguity in interpretation, however, does not hinder the general application of these ideas for the particular forecast problems of MCS maintenance and speed, as we will show in section 5.

4. RESULTS

a. MCS maintenance

This section examines the differences among selected variables between the mature and dissipation soundings. Although many of the differences of the wind shear variables (shear vector magnitudes, total shear, positive shear, etc.) between the mature and dissipation soundings are large, the greatest differences are among the shear vector magnitudes over very deep layers (Fig. 6). In fact, the deep-layer shear magnitudes have the largest Z-scores of *any* variable

tested. The deep-layer shear values (given in m s^{-1} over a given vertical layer) are larger for the mature soundings (Fig. 6), as suggested for derecho-producing MCSs alone by Coniglio et al. (2004). The differences in the low-level shear magnitudes are relatively small, suggesting that these values, alone, have limited utility in determining the stage of the MCS lifecycle.

The wind shear over a deep layer is perhaps the best discriminator because of the significant influence that mid-upper-level wind shear can have on the maintenance of MCSs (see section 2) along with the positive influences of the low-level shear on the initial organization and strength of the system (Weisman and Rotunno 2004). This suggests that an integrated measure of shear over a very deep layer has the most utility in forecasting the weakening of quasi-linear MCSs. Calculations of the total shear, or the hodograph length, which are correlated to the shear vector magnitudes, support this claim (not shown). Although the 0-10 km shear has the largest Z score among all of the wind shear variables, it is desirable to include a shear predictor in the logistic regression procedure that accounts for the possibility of variable heights of the low-level or upper-level jets that can control the effective depth and magnitude of the deep layer shear. Therefore, we define the "maximum deep shear" to be the maximum magnitude of the vector difference between any wind vector in the lowest 1 km and any wind vector in the 6-10 km layer. The Z-score for the maximum deep shear is slightly smaller than the Z-score for the 0-10 km shear, but still very large relative to the shallower shear variables.

We examine many variables related to instability including, but not limited to, several variations of CAPE, lapse rates over many layers, vertical differences in θ_e over many layers and find that the lapse rates over a deep portion of the convective cloud layer (generally from the lifting condensation level to some level in the 500 hPa to 300 hPa layer) are the most different among the mature and dissipation soundings. Although it is not surprising that larger lapse rates

are found for the more mature MCSs, the physical importance of the deeper, mid-level lapse rates versus the lower-level lapse rates is not obvious. One hypothesis is that steeper mid-level lapse rates make it easier for the shear in the convective cloud layer to maintain upright trajectories by allowing the convective updrafts to reach their vertical velocity potential earlier in the overturning process. This could lead to more cells that are placed close to the leading edge of the gust front compared to systems that occur in a smaller mid-level lapse rate environment. The 3-8 km lapse rate has the highest Z-score among the two groups, and is thus used as the primary instability variable in the logistic regression procedure. A discriminant analysis (Wilks 1995) between the two groups shows that the 3-8 km lapse rate, along with the maximum deep shear, separate 75% of the mature and dissipation soundings correctly (Fig. 7), which illustrates the potential utility of the deep shear and lapse rates in this context.

Among the other instability variables, we find that various CAPEs that are based on finding the most unstable mixed parcel over some layer tend to have large Z-scores between the mature and dissipation soundings and, interestingly, are only weakly correlated with the 3-8 km lapse rates. This appears to be because these CAPE variables are determined largely by the absolute moisture content in the layer with the maximum θ_e rather than the vertical temperature profile. The use of a CAPE variable in the logistic regression that is not tied to a particular level is desirable because this preserves the ability to represent systems that may be sustained by elevated inflow. This also allows for representing environments with "long, skinny" CAPE, in which the lapse rates may not be large, but the CAPE can still be significant if the equilibrium level pressure is very low. As illustrated later in section 5, the probability equations are applied using the Rapid Update Cycle (RUC) (Benjamin et al. 2003) output. Therefore, we use the

method of calculating the "best" CAPE in the RUC model as of this writing (hereafter denoted RCAPE) as the secondary instability predictor in the logistic regression. In this method, if the parcel with the maximum θ_e is found in the lowest 70 h Pa, the RCAPE is calculated from a mixed parcel in the lowest 70 h Pa; otherwise, the single most unstable parcel is used to calculate the CAPE (Stan Benjamin, personal communication).

In addition to the three variables mentioned above, the deep-layer mean wind speeds are very different between the mature and dissipation soundings. The 3-12 km mean wind speed has the largest Z-score among the mean wind variables and is used in the logistic regression procedure. The mean wind does not improve the discrimination substantially because of a moderate correlation with the maximum deep shear values. However, the inclusion of the mean winds allows for the possibility of representing environments that can support MCSs through mean wind/cold pool interactions (Evans and Doswell 2001) if the other processes are less important. These weaker shear/stronger mean wind environments appear to be more common to the MCS events that occur over the eastern third of the United States in our data set, although the relatively small sample size for these events prevents a definitive statement.

The four variables described above (maximum deep shear, 3-8 km lapse rate, RCAPE, 3-12 km mean wind speed) collectively separate over 80% of the soundings correctly when input into a discriminant analysis between the mature and dissipation soundings. It is worth noting that, because of the mutual correlations among the hundreds of variables, any additional variables provide negligible (< 1%) improvement on the discrimination of the two groups. Therefore, the maximum deep shear (*maxshear*), 3-8 km lapse rate (*3-8 lr*), RCAPE, and 3-12 km mean wind

(*3-12 mw*) are used as input to eq. (1) to develop the following equation for the MCS maintenance probability (MMP):

$$\underline{\underline{For\ RCAPE \geq 100\ J\ Kg^{-1}}}:$$

$$MMP = \frac{1}{\left[1 + EXP\left(a_0 + (a_1 * \{\max shear\}) + (a_2 * \{3 - 8\ lr\}) + (a_3 * \{RCAPE\}) + (a_4 * \{3 - 12\ mw\})\right)\right]} \quad (2)$$

$$\underline{\underline{For\ RCAPE < 100\ J\ Kg^{-1}}}:$$

$$MMP = 0,$$

where the regression coefficients are $a_0 = 13.0$ (dimensionless), $a_1 = -4.59 \times 10^{-2}$ m^{-1} s, $a_2 = -1.16$ C^{-1} km, $a_3 = -6.17 \times 10^{-4}$ J^{-1} kg, and $a_4 = -0.17$ m^{-1} s. Note that an RCAPE value below 100 J kg^{-1} zeros the MMP regardless of the other predictors.

Fig. 8 shows a plot of the equation for MMP for the four predictors that are normalized by their respective minimum and maximum values in the subset. As shown in Fig. 8, if all four of the predictors for the MMP are exactly half way between their minimum and maximum values (*maxshear* = 32 m s^{-1}, *3-8lr* = 6.6 C^{-1} km, *RCAPE* = 2980 J kg^{-1}, *3-12mw* = 22 m s^{-1}), then the regression equation predicts an 85% chance that the MCS will be strong and be maintained. Note that this is only one of many ways that a probability of 85% can be reached depending on the values of the predictors (for example, one particular sounding in the data set has *maxshear* = 42 m s^{-1}, *3-8lr* = 6.9 C km^{-1}, *RCAPE* = 383 J kg^{-1}, *3-12mw* = 21 m s^{-1}, and also has an MMP of 85%). The normalization of the variables in Fig. 8 is done to allow a smooth curve to be plotted so that the important point of the steepness of the curve for the MMP can be gained. In general, a steeper curve suggests a better ability to discriminate between the two groups and, therefore, the steepness of the curve suggests the potential for substantial skill in discriminating mature and weakening MCSs.

b. **MCS speed**

The same procedure described above is followed to identify the best discriminators between the 130 soundings in the $C < 18$ m s^{-1} group and the 98 soundings in the $C \geq 18$ m s^{-1} group. It is found that the low- to upper-level mean wind speeds are very good at discriminating between the two groups. Wind shear variables also discriminated well between the two groups, but not as well as the mean wind variables. It is tempting to conclude from this result that the mean wind speed, and its effects on the cold pool motion, has a more direct impact on the MCS forward-speed than the effects of the wind shear, as suggested by Evans and Doswell (2001) and Corfidi (2003), but the substantial correlations between the mean wind and wind shear variables prevents a firm conclusion on the relative physical importance of these two effects. Nonetheless, the mean wind speed over the 2-12 km layer has the highest Z-score, and thus is chosen to be the kinematic predictor variable for the development of the MCS speed probability equation.

The Z-scores for the thermodynamic variables, including CAPE, mean low-level mixing ratios, lapse rates, and vertical differences in θ_e, are relatively small, and thus did not provide a good discrimination between the two groups. However, the discrimination is improved by converting the variables into non-dimensional standard normal variables (Wilks 1995) based on their 7-year (1998-2004) mean and standard deviation derived from radiosonde data. This appears to result from a strong geographical signal in the data. For example, the $C \geq 18$ m s^{-1} soundings east of the Mississippi River have smaller lapse rates and deep vertical shear compared to the High-Plains events. The converse is true for the precipitable water values and mean low-level mixing ratios, as would be expected given the proximity to the Gulf of Mexico moisture source. These geographical differences in the variables are large enough so that the variables can't discriminate between the MCS speed categories when all the soundings east of

the Rocky Mountains are combined into one group. Therefore, a normalization of the thermodynamic variables is required to identify MCS speed predictors that can be applied over a wide geographical region.

Among the normalized variables, the maximum low- to mid-level difference in θ_e (*maxthediff ´*) and the lapse rates in the lower half of the cloud layer provide the best discrimination between the two groups. Based on these findings, *maxthediff ´*, the dimensional 2-12 km mean wind speed (m s^{-1}) (*2-12 mw*), and the normalized 2-6 km lapse rate (*2-6 lr ´*) are used as input to eq. (1) to generate an equation for the conditional probability that an MCS leading line will move with speeds ≥ 18 m s^{-1} (MSP), and is given by,

$$\underline{\underline{For\ RCAPE \geq 100\ J\ Kg^{-1}}}:$$

$$MSP = \frac{1}{\left[1 + EXP\left(a_0 + (a_1 * \{\max thediff'\}) + (a_2 * \{2-12\ mw\}) + (a_3 * \{2-6\ lr'\})\right)\right]} \qquad (3)$$

$$\underline{\underline{For\ RCAPE < 100\ J\ Kg^{-1}}}:$$

$$MSP = 0$$

where the regression coefficients are a_0 = -3.46 (dimensionless), a_1 = 0.447 (dimensionless), a_2 = 0.119 m^{-1} s, and a_3 = 0.79 (dimensionless). Although the regression curve for the MSP is not as steep as the curve for the MMP (Fig. 8), indicating a lesser degree of difference identified between the C < 18 m s^{-1} and C ≥ 18 m s^{-1} groups, the slope of the curve still suggests some ability to discriminate between "slow" and "fast" MCSs. Fig. 8 shows that if the three predictors are exactly half way between their minimum and maximum values in the subset (*maxthediff ´* = 1.15, *2-12mw* = 21 m s^{-1}, *2-6lr ´* = 0.48), then the MCS leading line has a 50% chance of attaining a speed ≥ 18 m s^{-1}.

c. Application of the probability equations

We envision the best real-time application of the probability equations would use observational data or short-term model output at a time close to convective initiation. For example, gridded fields from the hourly RUC can be used to calculate these probabilities and give guidance to the regions most likely to sustain strong MCSs that do develop (this is illustrated later in this section). This could benefit Day 1 Severe Weather Outlooks, Mesoscale Discussions, and the issuance of Severe Weather Watches at the SPC, and short-term forecasts issued by local forecast offices. Additionally, although the probability equations are designed primarily to discriminate between mature and weakening MCSs that are imminent or ongoing, it may also be used with mesoscale model output well before convective initiation to give an idea of where strong, mature MCSs may be favored on longer time scales, assuming convection in the model doesn't remove instability erroneously.

A small collaborative program recently took place during the summer of 2005 at the SPC and the National Severe Storms Laboratory (NSSL) as part of the National Oceanic Atmospheric Administration Hazardous Weather Testbed to test the ability of these conditional probability forecasts to provide useful guidance to forecasters at the SPC (see http://www.nssl.noaa.gov/hwt/ for more information). To meet the goals of this program, daily activities included the documentation of MCSs using national mosaic radar reflectivity and the evaluation of the probabilities calculated using the hourly RUC forecasts.

Examples of the MMP and MSP generated from operational RUC model output are illustrated for a derecho MCS that occurred on 2-3 July 2005 (Fig. 9). The MCS developed a broad bowing signature in its early stages and was composed of smaller-scale embedded bow echoes that were responsible for several reports of wind gusts > 33 m s^{-1} in western South

Dakota. The wind reports became less frequent as the MCS expanded in size and the leading line exhibited less bowing characteristics after 0800 UTC. During its lifetime, the MCS moved at speeds of 20-22 m s^{-1}, but slowed to 15-17 m s^{-1} in the last few hours of its existence, which coincided with a rapid weakening of the 50+ dBZ echoes within the leading line.

The RUC 3 h forecasts generate MMPs over 90% in the region of the MCS for much of its lifecycle (Fig. 10a). The spatial configuration of the MMP values changes little throughout the 12 h forecast cycle so that the 3 h forecast provides a good representation of the MMP at the other forecast hours. The MMP signals the weakening of the northern half of the MCS after 0800 UTC in western and north-central Minnesota as the probabilities decrease to 30-40% in this region. The MMP values also provide useful guidance on the overall MCS dissipation by 1200 UTC in southeastern Minnesota as the MMP values quickly drop to 10% in this area.

The MSPs suggest the persistence of a favorable environment for the system to attain speeds $\geq$ 18 m s^{-1} as the MSPs are 60-70% in much of the area that the MCS traverses (Fig. 10b). In addition, the MSPs drop to 20-30% where the system slows to speeds < 18 m s^{-1} toward the end of its lifecycle over southern Minnesota.

The above example illustrates a successful application of the probability equations with short-term numerical model output. Although the analyses of the data collected during the SPC/NSSL Summer Program are preliminary at the time of this writing, the equations appear to satisfy the goals of this study to provide useful guidance on the transition of system with a solid line of 50+ dbZ echoes to a more disorganized system with unsteady changes in structure and propagation characteristics. This speaks to the potential of these probability equations to particular forecast problems, despite the ambiguity in their interpretation discussed earlier.

Because of the relationship between systems with a solid line of strong echoes to the production of severe surface winds, we also find that the MMP used together with the MSP values may be able to guide forecasters on the cessation of severe surface winds. This is illustrated next with a supercell/MCS event that occurred between 0000 - 1400 UTC on 1 July 2005 in the central and southern Plains region (Fig. 11). A nearly stationary synoptic front meandered from the Front Range of the Colorado Rockies southward into far northeastern New Mexico, then stretched eastward across the Texas Panhandle and eventually northeastward toward the central Mississippi River valley. Isolated convection developed in east-central Colorado during the late afternoon of 30 June and developed into a supercell that moved through southeastern Colorado and southwestern Kansas from 0200 to 0600 UTC (Fig. 11). Although northeasterly surface winds were found up to ~750 h Pa north of the front in the 0000 UTC Dodge City sounding (not shown), the boundary layer was well-mixed and supported surface winds exceeding 40 m s^{-1} with the upscale growth of the supercell. The supercell then continued to grow upscale and developed linear characteristics as it entered Oklahoma by 0700 UTC, with a continuation of the severe surface winds north of the front (Fig. 11).

Although forecasters were aware of the potential for severe winds in this region, the persistence and strength of the convectively-induced surface winds north of the front were not anticipated. Given that the CAPE, deep shear, and mid-level lapse rates are relatively large in the RUC forecasts, the MMP values suggest the persistence of a strong, quasi-linear system with values of 70-90% in the region that the supercell transitioned to an MCS in southwestern Kansas and northwestern Oklahoma (Fig. 12a). The MSP values indicated a > 50% chance of an MCS moving greater than 18 m s^{-1} in this region (Fig. 12b). It is intriguing that the area that experienced the severe surface winds was confined to the region of higher MMP and MSP

values, which could have been used to signal the potential for an organized and fast-forward propagating system. This could have steered forecasters to examine this area for the potential for organized severe surface winds more critically, despite the location of the system well north of the front in a region of northeasterly low-level flow.

Just as important, and perhaps the more challenging aspect of the forecast, was the cessation of the severe surface winds and the weakening of the convective system once it entered the warm sector air (Fig. 11). The line underwent changes in structure and showed characteristics of discrete forward propagation as it crossed the frontal zone. The line then reorganized temporarily into a weaker linear system before dissipating altogether in eastern Oklahoma by 1400 UTC (Fig. 11). Just as the MMP values could have increased the awareness of an organized severe wind threat in southwestern Kansas and far northwestern Oklahoma, the MMP values could have alerted forecasters to the decreasing probability of an organized system across northwestern and central Oklahoma with values dropping quickly to 10-20% across this region (Fig. 12a). A similar, but less dramatic drop is seen with the MSP values in central and eastern Oklahoma (Fig. 12b). Maximum deep shear values that drop quickly from over 35 m s^{-1} over the Oklahoma Panhandle to less than 20 m s^{-1} across west-central Oklahoma and RCAPE values that drop below 1000 J kg^{-1} (not shown) appear to dictate the rapid drop in the MMP in this case.

5. SUMMARY AND DISCUSSION

This paper addresses the problem of predicting the speed and maintenance of MCSs that obtain a quasi-linear or arced leading edge of deep convection for several hours. Environmental variables that best differentiate between mature and weakening MCSs, as well as between MCSs that travel slower or faster than 18 m s^{-1} are identified from a large set of observed proximity soundings. The goal is to use these variables to develop equations that provide probabilistic

guidance on MCS speed and maintenance. A fitting method of calculating probabilities in this context is logistic regression, which provides an equation that gives the probability of one of two groups occurring.

For the discrimination of mature and weakening MCS environments, the vertical wind shear over very deep layers is found to be the variable with the largest statistical differences. Some possible physical mechanisms for this difference are summarized in Section 2. Lapse rates over a significant depth of the convective cloud layer, the maximum mixed-layer CAPE, and low-to-upper level mean wind speeds also discriminate between mature and weakening MCSs very well.

The low-to-upper level mean wind speeds provide the largest statistical differences between the "slow" and "fast" MCS environments. Additionally, normalized values of low-to-mid level lapse rates and low-to-mid level differences in θ_e also discriminate these environments very well.

Two examples illustrate that the logistic regression equations based on these predictors and used with short-term numerical model output can provide useful guidance on the transition of a system with a solid line of 50+ dbZ echoes to a more disorganized system with unsteady changes in structure and propagation characteristics. A more indirect, but equally useful application may be on the potential for an MCS to produce severe surface winds on regional scales.

We are also mindful of limitations of the probability equations and, to that end, in the use of cold pool/shear/mean wind concepts for the forecasting of MCSs in general. In summary, we have found that once MCSs become established, the deeper layer wind shear tends to provide a better indicator of MCS maintenance than low-level-only shear variables. We have also found that decreasing lapse rates in the lower half of the convective cloud layer appear to be excellent predictors of a weakening MCS. This appears to be especially true of the cases that mature in the larger deep-shear/larger lapse-rate regimes that typify severe weather episodes in the central

United States during the warm season, as in the examples shown above. We emphasize that the probabilities developed in this paper and these concepts in general will likely work best on MCSs that develop and continually generate strong cold pools away from larger-scale forcing when the shear and mean winds are substantial. However, MCSs can maintain coherence through other means, including discrete propagation along a surging outflow (one such case occurred with an MCS on 30 June 2005 in the Ohio Valley), frontogenetic circulations, gravity-wave interactions, and other larger-scale forcing mechanisms, in which the probability equations may not be as applicable. Regarding these other MCS modes, we will report on the overall performance of the equations documented during the Summer Program in a future paper.

It should be noted again that the probability equations are designed with the goals of the SPC in mind, particularly with the issuance of the Day 1 convective outlooks and watches along MCS tracks. We recognize that the convective-scale details of the evolution, especially the low-level vertical thermodynamic structures of the system and the environment, ultimately dictate the county-scale locations of severe surface winds. Accurate prediction at these scales likely will await advances in either the ability to observe the fine-scale details of the low-level moisture and advances in the prediction of these systems with numerical weather prediction schemes that assimilate convective-scale observations (Dowell et al. 2004). But the examples presented above illustrate that forecast tools based on environmental variables and their statistical relationships still have the potential to provide forecasters with improved information on the qualitative characteristics of MCS structure and longevity, and perhaps refined information on the potential for severe weather on regional scales. We urge the meteorological community to continue to undertake studies of this type while we move forward into the era of convective-scale data assimilation using convection-resolving numerical weather prediction models.

ACKNOWLEDGMENTS

The SPC/NSSL 2005 Summer Program would not have been possible without the help of David Bright and Jay Liang of the SPC. We thank the SPC forecasters and the NSSL scientists who have volunteered their time to participate in the program. We are also grateful to Bob Johns for contributing his time and wealth of knowledge and experience to this project. We thank Drs. Matt Parker and Robert Fovell for the helpful discussions regarding the background material for this paper. This project was supported through a National Research Council Postdoctoral Award for the first author under the guidance of the second author.

REFERENCES

Benjamin, S.G. and others, 2003: An hourly assimilation-forecast cycle: The RUC. *Mon. Wea. Rev.*, 132, 495-518.

Bryan, G., D. Ahijevych, C.A. Davis, and M.L. Weisman, 2005: Observations of cold pool properties in mesoscale convective systems during BAMEX. Preprints, *32nd Conf. on Mesoscale Meteorology*, Albuquerque, NM, CD-ROM.

Chappell, C.F., 1986: Quasi-stationary convective events. Mesoscale Meteorology and Forecasting, P. Ray, Ed., Amer. Meteor. Soc., 289-310.

Cohen, A.E., M.C. Coniglio, S.F. Corfidi, and S.J. Taylor, 2006: Discrimination among non-severe, severe, and derecho-producing mesoscale convective systems. Preprints, *86th Amer. Meteor. Soc. Annual Meeting*, CD-Rom.

Coniglio, M.C., and D.J. Stensrud, 2001: Simulation of a progressive derecho using composite initial conditions. *Mon. Wea. Rev.*, **129**, 1593-1616.

--------, --------, and M.B. Richman, 2004: An observational study of derecho-producing convective systems. *Wea. Forecasting*, **19**, 320-337.

--------, L.J. Wicker, and D.J. Stensrud, 2005: Effects of upper-level shear on the structure and maintenance of strong quasi-linear mesoscale convective systems. *J. Atmos. Sci.*, accepted for publication.

Corfidi, S.F., 2003: Cold pools and MCS propagation: Forecasting the motion of downwind-developing MCSs. *Wea. Forecasting*, **18**, 997-1017.

Cotton, W.R., M.-S. Lin, R.L. McAnelly, and C.J. Tremback, 1989: A composite model of mesoscale convective complexes. *Mon. Wea. Rev*., **117**, 765-783.

Davis, C.A., N. Atkins, D. Bartels, L.F. Bosart, G. Byran, M. Coniglio, W. Cotton, D.Dowell, B.Jewett, R.Johns, D. Jorgensen, J. Knievel, K. Knupp, W. Lee, G. Mcfarquhar, J. Moore, R. Przybylinski, R. Rauber, B. Smull, R. Trapp, S. Trier, R. Wakimoto, M. Weisman and C. Ziegler, 2004: The Bow-Echo and MCV experiment (BAMEX): Observations and Opportunities. *Bull. Amer. Meteor. Soc.,* **85**, 1075-1093.

Dowell, D.C., F. Zhang, L.J. Wicker, C. Snyder, and N.A. Crook, 2004: Wind and temperature retrievals in the 17 May 1981 Arcadia, Oklahoma, supercell: Ensemble Kalman filter experiments. *Mon. Wea. Rev*., **132**, 1982-2005.

Evans, J.S., and C.A. Doswell, 2001: Examination of derecho environments using proximity soundings. *Wea. Forecasting*, **16,** 329-342.

Fovell, R. G. and P.S. Daily, 1995: The temporal behavior of numerically simulated multi-cell type storms. Part I: Modes of behavior. *J. Atmos. Sci.*, **52**, 2073-2095.

--------, B. Rubin-Oster, and S. Kim, 2005: A discretely propagating nocturnal Oklahoma squall line: Observations and numerical simulations. Preprints, *22nd Conf. on Severe Local Storms*, Hyannis, MA, CD-ROM.

Fritsch J.M. and G.S. Forbes, 2001: Mesoscale convective systems. *Severe Convective Storms*, *AMS Meteor. Monogr.*, C. Doswell III, Ed., **28**, Amer. Meteor. Soc., 323-357.

Gale, J.J., W.A. Gallus Jr., and K.A. Jungbluth, 2002: Toward improved prediction of mesoscale convective system dissipation. *Wea. Forecasting*, **17**, 856-872.

Kain. J.S., S.J. Weiss, M.E. Baldwin, G.W. Carbin, D. Bright, J.J. Levit, and J.A. Hart, 2005: Evaluating high-resolution configurations of the WRF model that are used to forecast severe convective weather: The 2005 SPC/NSSL Spring Experiment. Preprints, *21st Conf. on Weather Analysis and Forecasting*, Amer. Meteor. Soc., Washington, D.C. paper 2A.5.

Klimowski, B.A., M.J. Bunkers, M.R. Hjelmfelt, and J.N. Covert, 2003: Severe convective windstorms over the northern High Plains of the United States. Wea. Forecasting, 18, 502-519.

Moncrieff, M.W. and C. Liu, 1999: Convection initiation by density currents: Role of convergence, shear, and dynamical organization. *Mon. Wea. Rev*., **127**, 2455-2464.

Parker, M.D., and R.H. Johnson, 2000: Organizational modes of midlatitude mesoscale convective systems. *Mon. Wea. Rev*., **128**, 3413-3436.

--------, and --------, 2004a: Structures and dynamics of quasi-2D mesoscale convective systems. *J. Atmos. Sci.*, **61**, 545-567.

--------, and --------, 2004b: Simulated convective lines with leading precipitation. Part I: Governing dynamics. *J. Atmos. Sci.*, **61**, 1637-1655.

--------, and --------, 2004c: Simulated convective lines with leading precipitation. Part II: Evolution and maintenance. *J. Atmos. Sci.*, **61**, 1656-1673.

Seitter, K. L., 1986: A numerical study of atmospheric density current motion including the effects of condensation. *J. Atmos. Sci.,* **43**, 3068–3076.

Shapiro, A., 1992: A hydrodynamical model of shear flow over semi-infinite barriers with application to density currents. *J. Atmos. Sci*., **49**, 2293-2305.

Stensrud D.J., M.C. Coniglio, R. Davies-Jones, and J. Evans, 2005: Comments on "'A theory for strong long-lived squall lines' revisted ". *J. Atmos. Sci.*, **62**, 2989-2996.

Trier, S.B. and C.A. Davis, 2005: Propagating nocturnal convection within a 7-day WRF-model simulation. Preprints, *32nd Conf. on Mesoscale Processes*, Amer. Meteor. Soc., CD-ROM.

Weisman, M.L., and R. Rotunno, 2004: "A theory for strong, long-lived squall lines" revisted. *J. Atmos. Sci*., **61**, 361-382.

Wilks, D.S., 1995: *Statistical Methods in the Atmospheric Sciences*. Academic Press, 467 pp.

Zipser, K.A, 1982: Use of a conceptual model of the life cycle of mesoscale convective systems to improve very-short-range forecasts. *Nowcasting*, K. Browning, Ed., Academic Press, 191-204.

FIGURE CAPTIONS

Fig. 1. Schematic depiction of a multicellular cycle within a convective system in deep shear. (a) Development of a fresh updraft at the outflow boundary/gust front; (b) maturation of the overturning updraft; (c) the updraft is cut off from the inflow by precipitation. The cold pool and cloud outlines are shown schematically, along with typical airstreams. The LFC and orientation of the deep tropospheric shear vector are also shown. In (b), the shaded region represents the mesoscale region of positive buoyancy associated with the line-leading cloudiness. In (c), the shaded region represents the newly developed convective precipitation cascade. Pressure maxima and minima are shown with "H" and "L" characters; their sizes indicate approximate magnitudes and their subscripts indicate the pressure components to which they are attributed (B - buoyancy, DL - dynamic linear, DNL – dynamic nonlinear). The vertical scale is expanded somewhat below the LFC and contracted somewhat above the LFC (from Parker and Johnson 2004b).

Fig. 2. Distributions of the maximum vertical displacements of several hundred parcels that pass through the deep convective regions of simulated convective systems within various values of 5-10-km shear (all of the simulations had a fixed value of 20 m s^{-1} of shear over 0-5 km). The lines extend to the 10^{th} and 90^{th} percentiles and the boxes enclose the interquartile range (25^{th} and 75^{th} percentiles). The thin lines within each box represent the median (from Coniglio et al. 2005).

Fig. 3. Cross section from the 10 June 2003 bow echo MCS produced from quad-Doppler analysis. Shown are system-relative winds and reflectivity (dbZ) in the vertical plane (from Davis et al. 2004).

Fig. 4. Special sounding launched at 0243 UTC 10 June 2003 in the environment ahead of the bow echo MCS (obtained from http://www.joss.ucar.edu/bamex/catalog).

Fig. 5. The number and locations of soundings used in this study.

Fig. 6. Median shear vector magnitudes (lines marked X) calculated over various depths among the mature (black) and dissipation (grey) sounding groups. The thin lines enclose the 25^{th} and 75^{th} percentiles for each distribution.

Fig. 7. Scatterplot of the maximum deep shear (m s^{-1}) versus the 3-8 km lapse rate (C km^{-1}) for the mature and dissipation soundings. The linear discrimination line separates 75% of the soundings correctly.

Fig. 8. Probability of MCS maintenance (MMP, solid line) and MCS speed ≥ 18 m s^{-1} (MSP, dashed line) based on logistic regression. The ordinate represents the predictors normalized by their minimum and maximum values in the data subset. For example, if all four of the predictors for the equation for MCS maintenance are exactly half way between their minimum and maximum values (0.5), then the regression equation predicts a ~85% chance that the MCS will be maintained. In dimensional values, this corresponds to a maximum deep shear of 32 m s^{-1}, a 3-8 km lapse rate of 6.6 C^{-1} km, a RCAPE of 2980 J kg^{-1}, and a 3-12 km mean wind speed of 22

m s^{-1}. In general, a steeper curve means a better ability of the parameters to discriminate between the two groups.

Fig. 9. Hourly traces of the leading edge of the nearly contiguous area of 35+ dBZ echoes associated with the MCS on 2-3 July 2005 (solid lines). Times (UTC) of the traces are labeled on the line and the dates (YYYYMMDD) are shown for the first and last trace. The letters represent severe weather reports from 1200 UTC on 2 July 2005 to 1159 UTC on 3 July 2005 (g – severe wind gust, w- severe wind, a – severe hail, t – tornado). Capital letters represent "significant" reports (33+ m s^{-1} wind or 5+ cm diameter hail).

Fig. 10. (a) Values of the MCS maintenance probability (%) based on a 3-h RUC forecast valid at 0300 UTC 3 July 2005. (b) As in (a), except for the MCS speed probability ≥ 18 m s^{-1} (%).

Fig. 11. Surface chart valid 0600 UTC on 1 July 2005 produced by the National Center for Environmental Prediction. Solid grey lines denote the hourly positions of the leading edge of the 50+ dbz echoes associated with the supercell and MCS from 0200 UTC to 1400 UTC. "W" denotes the locations of severe wind reports.

Fig. 12. (a) Values of the MCS maintenance probability (%) based on a 6-h RUC forecast valid at 0600 UTC 1 July 2005. (b) As in (a), except for the probability of MCS speed ≥ 18 m s^{-1}(%).

FIGURES

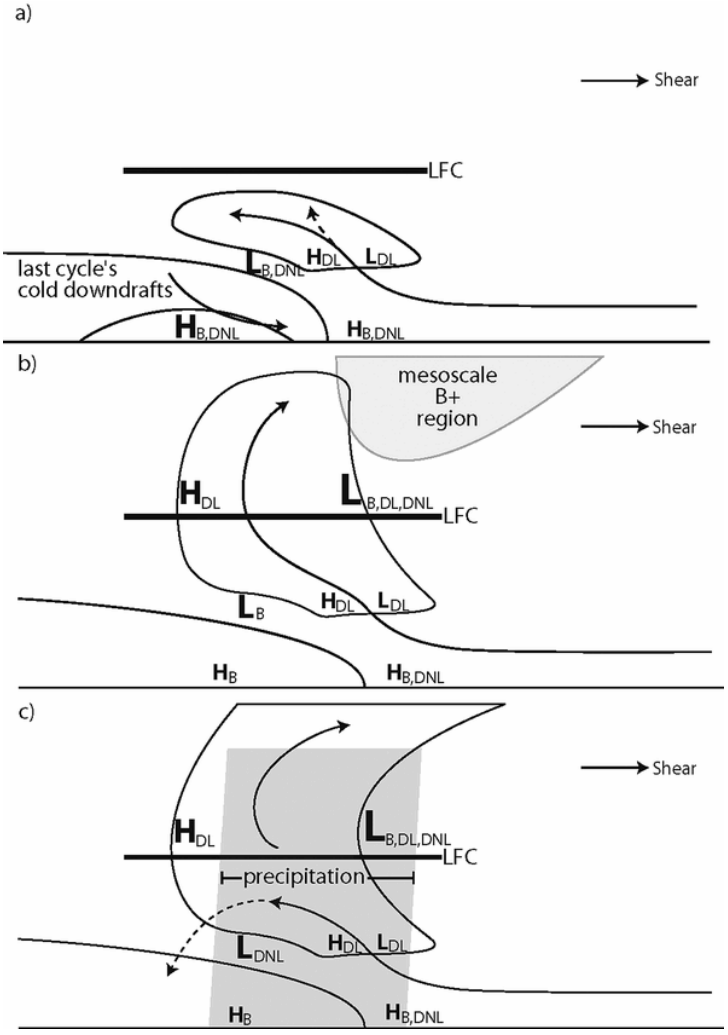

Fig. 1. Schematic depiction of a multicellular cycle within a convective system in deep shear. (a) Development of a fresh updraft at the outflow boundary/gust front; (b) maturation of the overturning updraft; (c) the updraft is cut off from the inflow by precipitation. The cold pool and cloud outlines are shown schematically, along with typical airstreams. The LFC and orientation of the deep tropospheric shear vector are also shown. In (b), the shaded region represents the mesoscale region of positive buoyancy associated with the line-leading cloudiness. In (c), the shaded region represents the newly developed convective precipitation cascade. Pressure maxima and minima are shown with "H" and "L" characters; their sizes indicate approximate magnitudes and their subscripts indicate the pressure components to which they are attributed (B - buoyancy, DL - dynamic linear, DNL – dynamic nonlinear). The vertical scale is expanded somewhat below the LFC and contracted somewhat above the LFC (from Parker and Johnson 2004b).

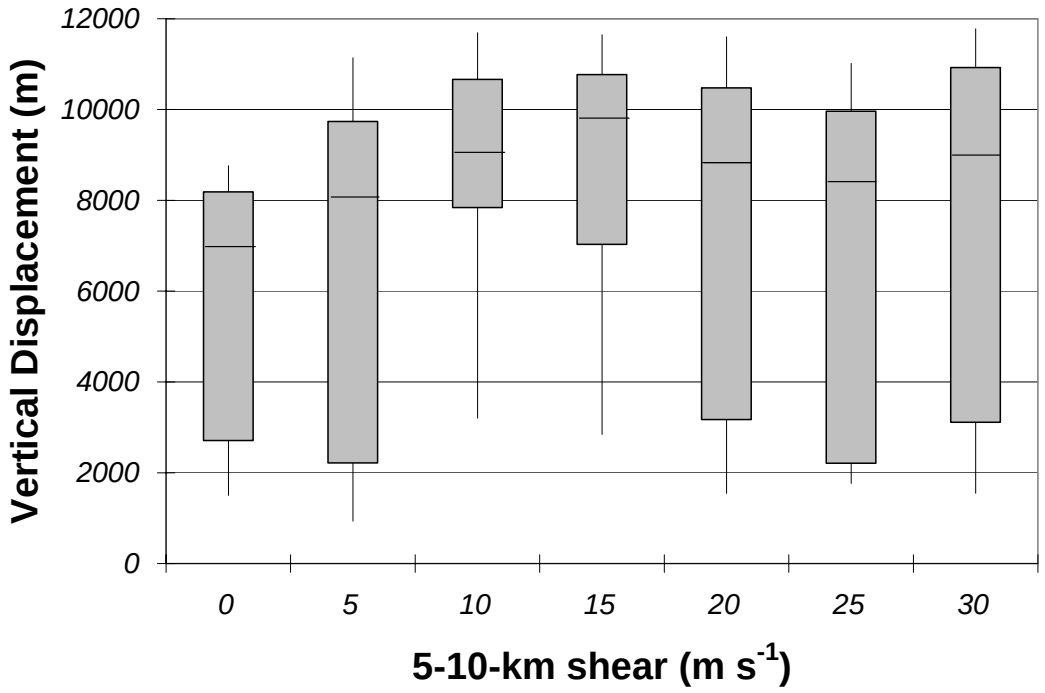

Fig. 2. Distributions of the maximum vertical displacements of several hundred parcels that pass through the deep convective regions of simulated convective systems within various values of 5-10-km shear (all of the simulations had a fixed value of 20 m s^{-1} of shear over 0-5 km). The lines extend to the 10^{th} and 90^{th} percentiles and the boxes enclose the interquartile range (25^{th} and 75^{th} percentiles). The thin lines within each box represent the median (from Coniglio et al. 2005).

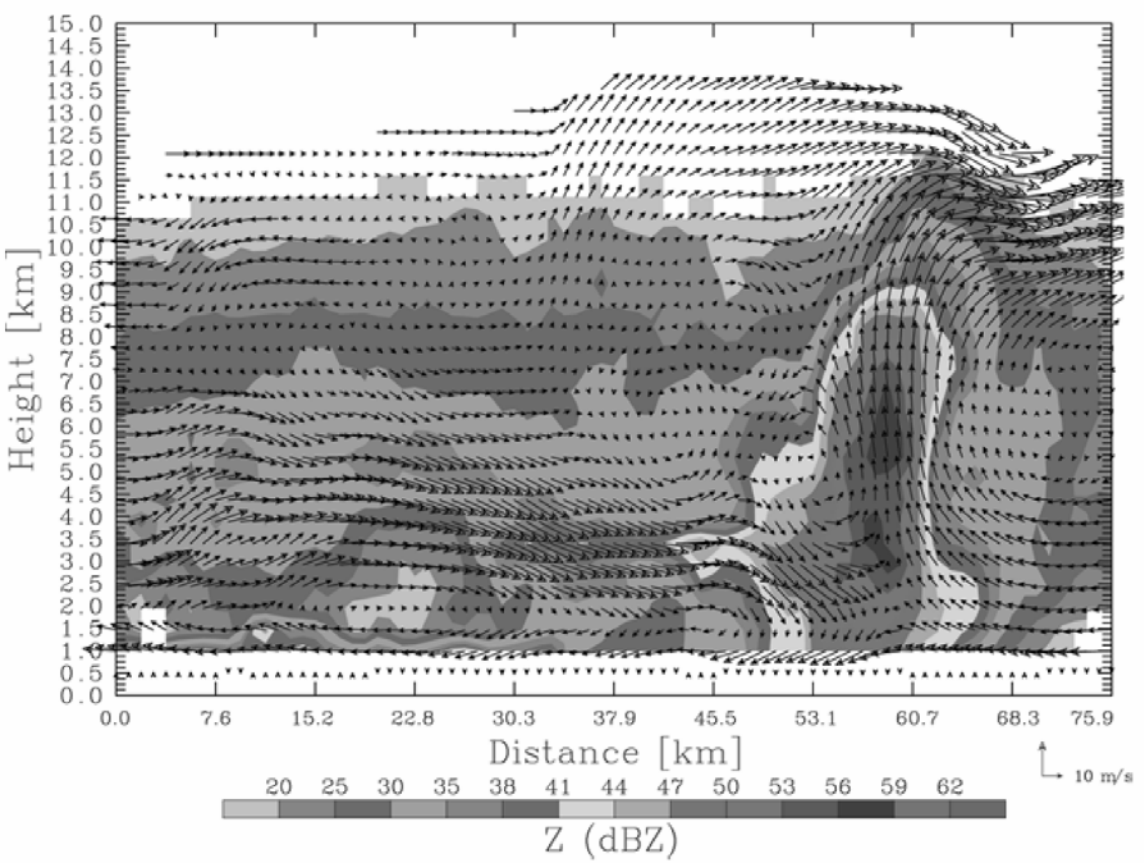

Fig. 3. Cross section from the 10 June 2003 bow echo MCS produced from quad-Doppler analysis. Shown are system-relative winds and reflectivity (dbZ) in the vertical plane (from Davis et al. 2004).

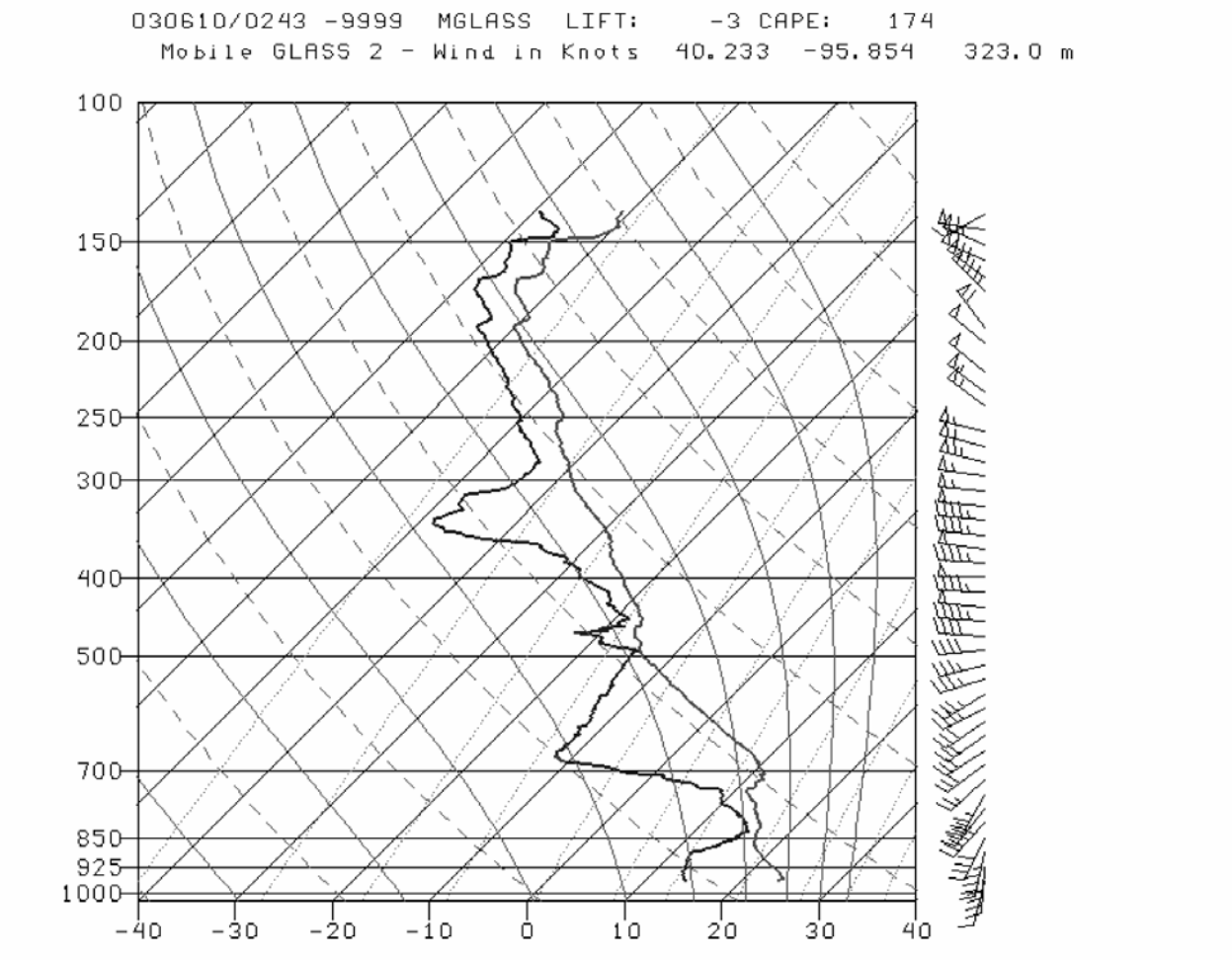

Fig. 4. Special sounding launched at 0243 UTC 10 June 2003 in the environment ahead of the bow echo MCS (obtained from http://www.joss.ucar.edu/bamex/catalog).

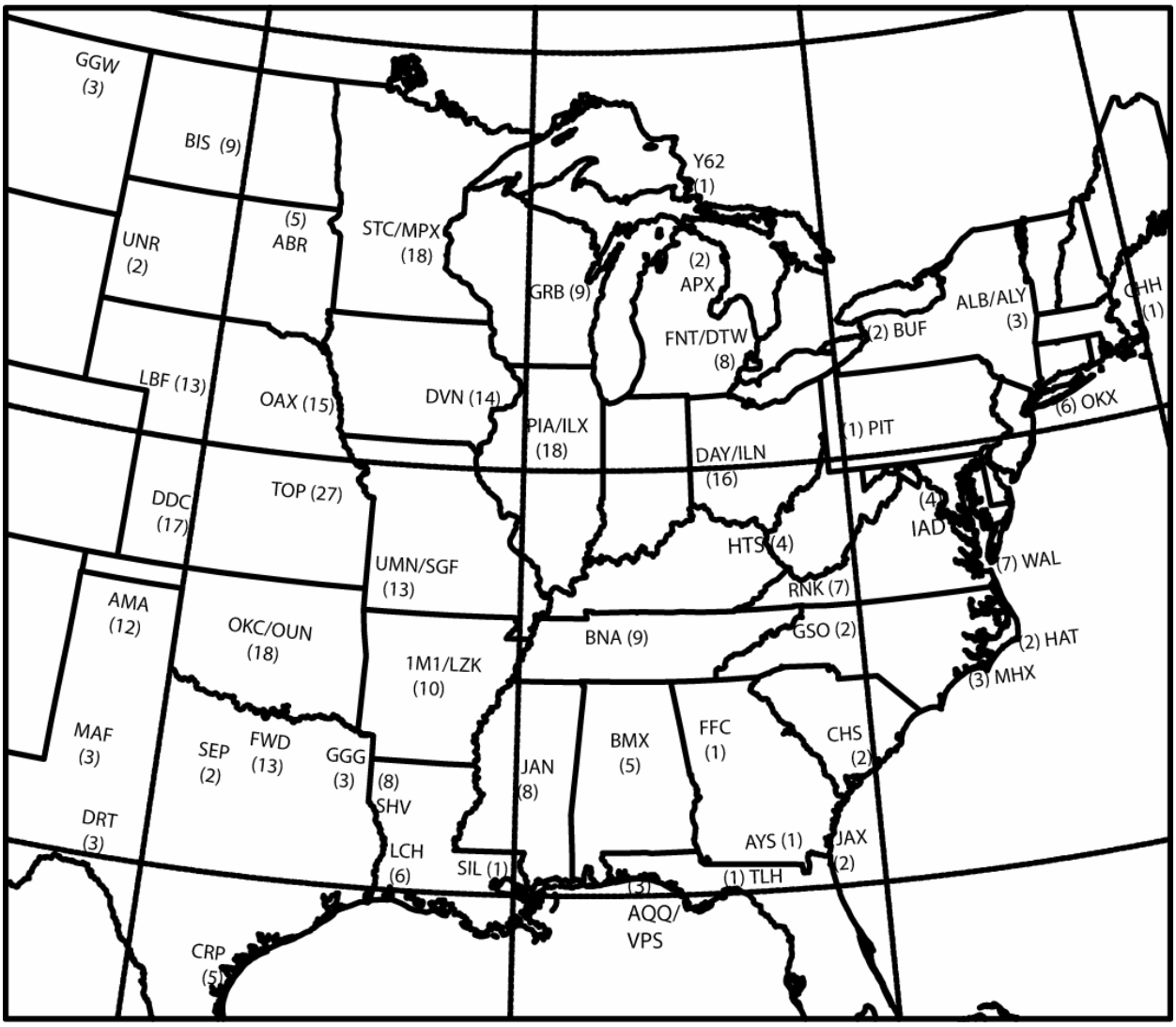

Fig. 5. The number and locations of soundings used in this study.

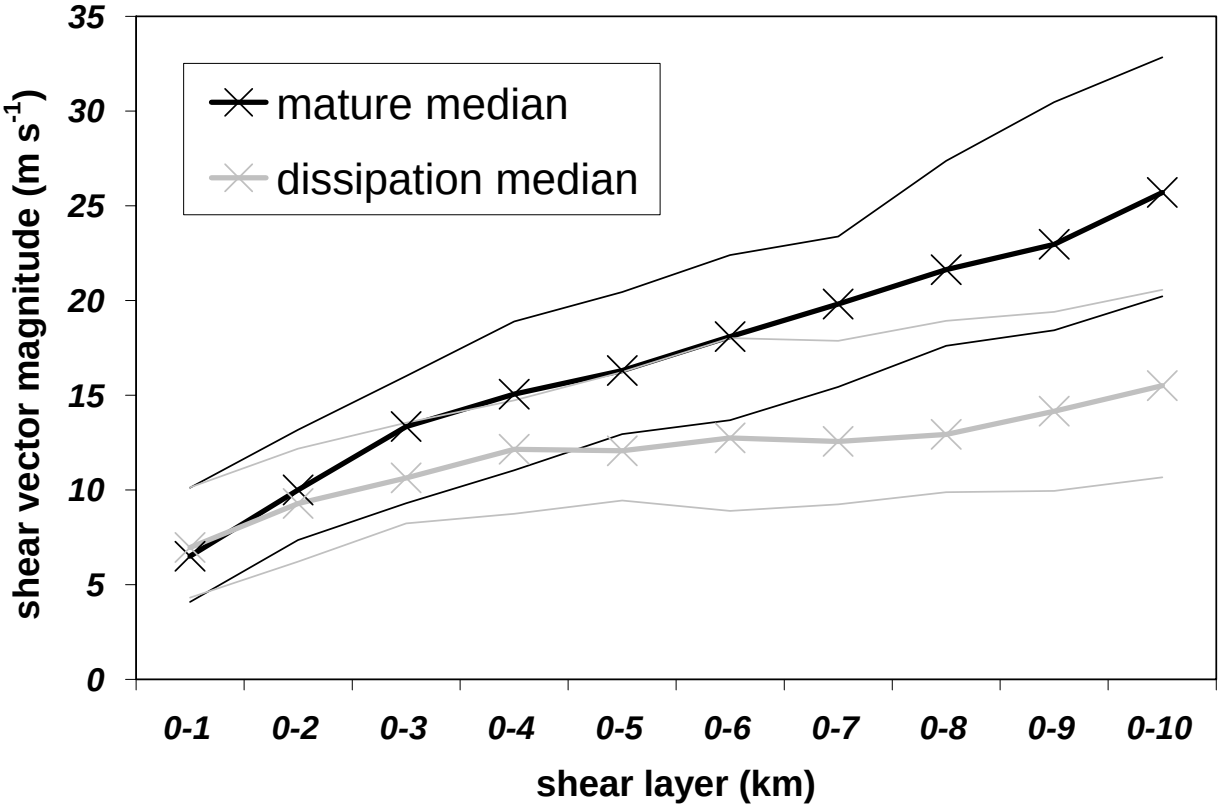

Fig. 6. Median shear vector magnitudes (lines marked X) calculated over various depths among the mature (black) and dissipation (grey) sounding groups. The thin lines enclose the 25th and 75th percentiles for each distribution.

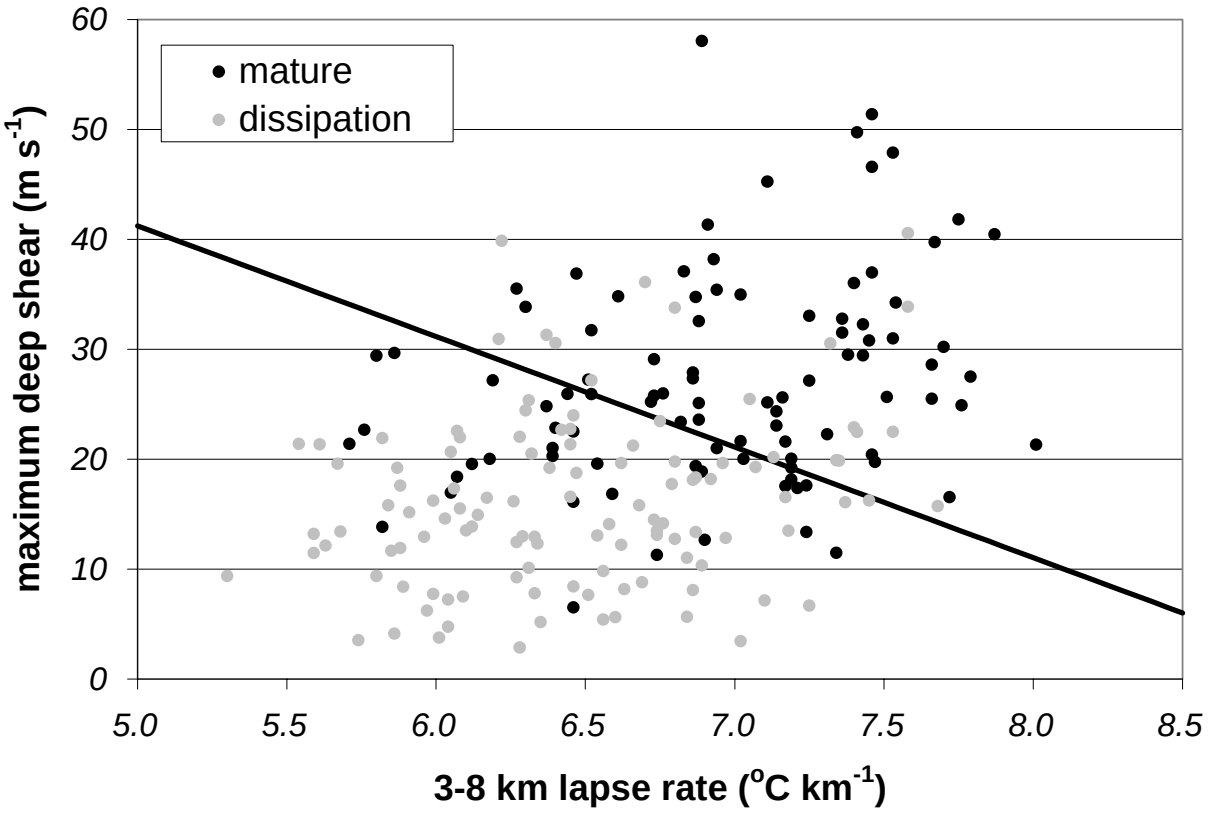

Fig. 7. Scatterplot of the maximum deep shear (m s^{-1}) versus the 3-8 km lapse rate (C km^{-1}) for the mature and dissipation soundings. The linear discrimination line separates 75% of the soundings correctly.

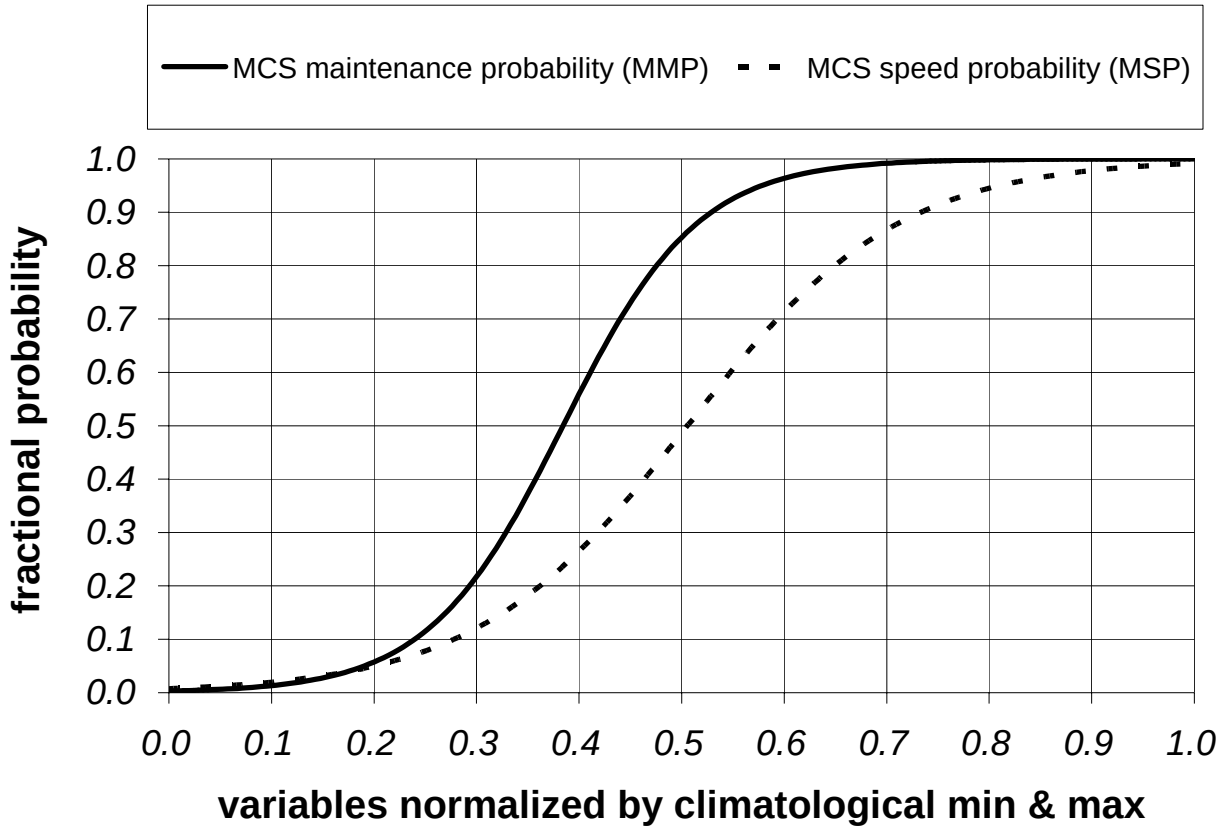

Fig. 8. Probability of MCS maintenance (MMP, solid line) and MCS speed ≥ 18 m s^{-1} (MSP, dashed line) based on logistic regression. The ordinate represents the predictors normalized by their minimum and maximum values in the data subset. For example, if all four of the predictors for the equation for MCS maintenance are exactly half way between their minimum and maximum values (0.5), then the regression equation predicts a ~85% chance that the MCS will be maintained. In dimensional values, this corresponds to a maximum deep shear of 32 m s^{-1}, a 3-8 km lapse rate of 6.6 C^{-1} km, a RCAPE of 2980 J kg^{-1}, and a 3-12 km mean wind speed of 22 m s^{-1}. In general, a steeper curve means a better ability of the parameters to discriminate between the two groups.

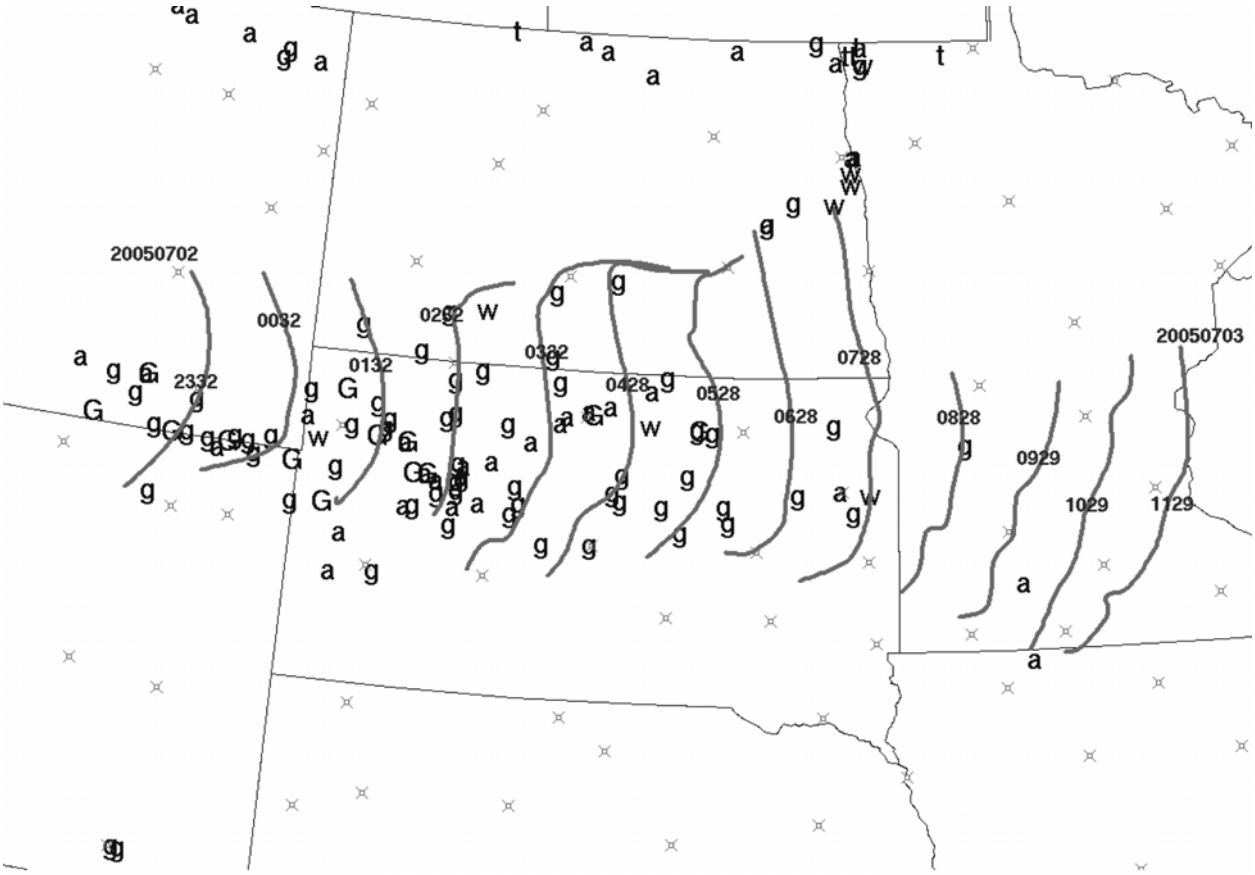

Fig. 9. Hourly traces of the leading edge of the nearly contiguous area of 35+ dBZ echoes associated with the MCS on 2-3 July 2005 (solid lines). Times (UTC) of the traces are labeled on the line and the dates (YYYYMMDD) are shown for the first and last trace. The letters represent severe weather reports from 1200 UTC on 2 July 2005 to 1159 UTC on 3 July 2005 (g – severe wind gust, w- severe wind, a – severe hail, t – tornado). Capital letters represent "significant" reports (33+ m s^{-1} wind or 5+ cm diameter hail).

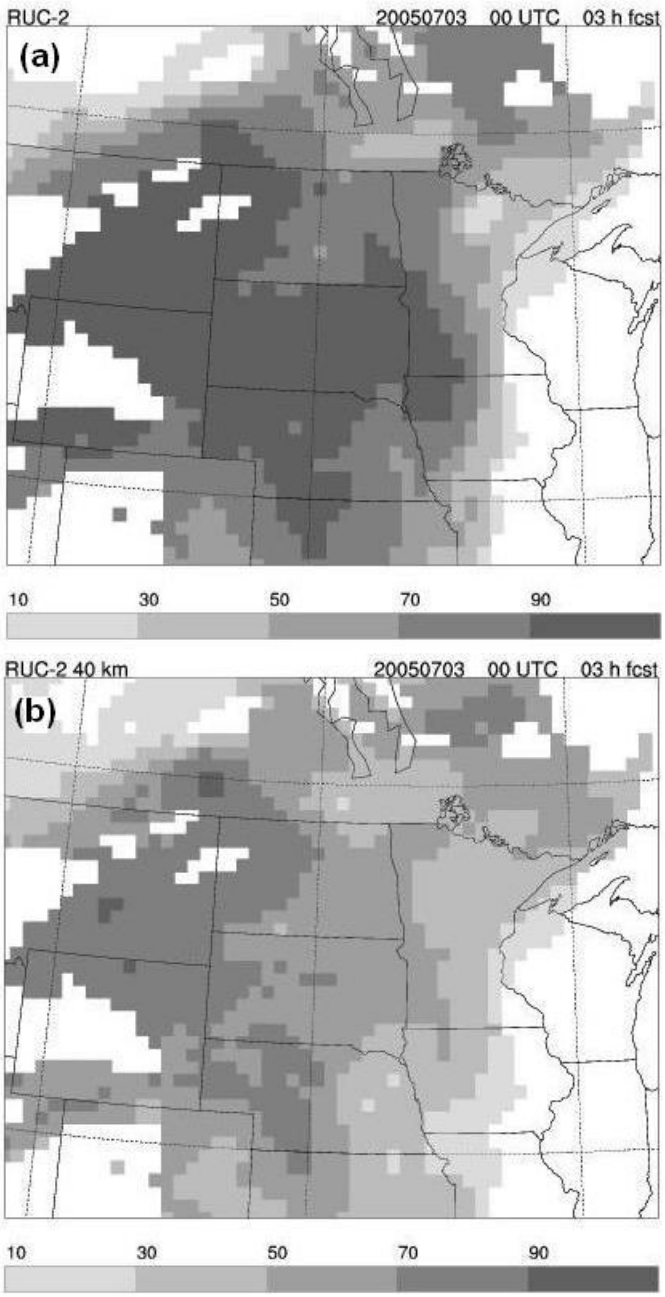

Fig. 10. (a) Values of the MCS maintenance probability (%) based on a 3-h RUC forecast valid at 0300 UTC 3 July 2005. (b) As in (a), except for the MCS speed probability ≥ 18 m s^{-1} (%).

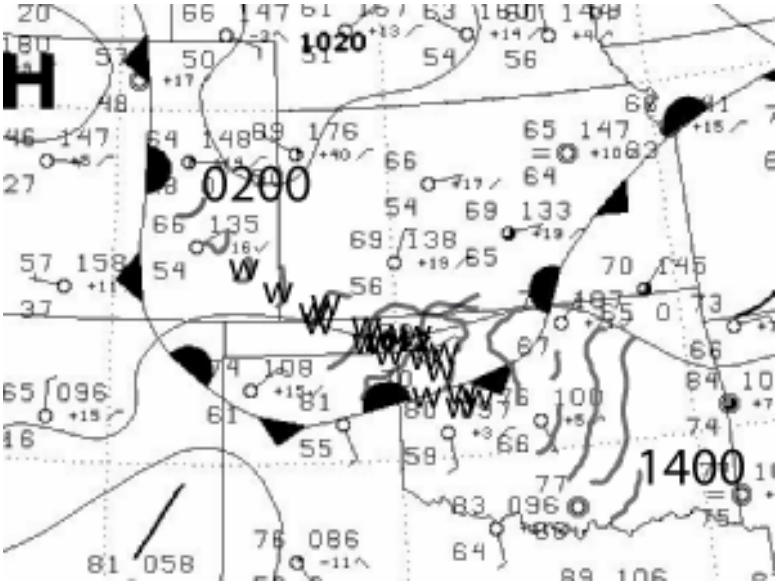

Fig. 11. Surface chart valid 0600 UTC on 1 July 2005 produced by the National Center for Environmental Prediction. Solid grey lines denote the hourly positions of the leading edge of the 50+ dbz echoes associated with the supercell and MCS from 0200 UTC to 1400 UTC. "W" denotes the locations of severe wind reports.

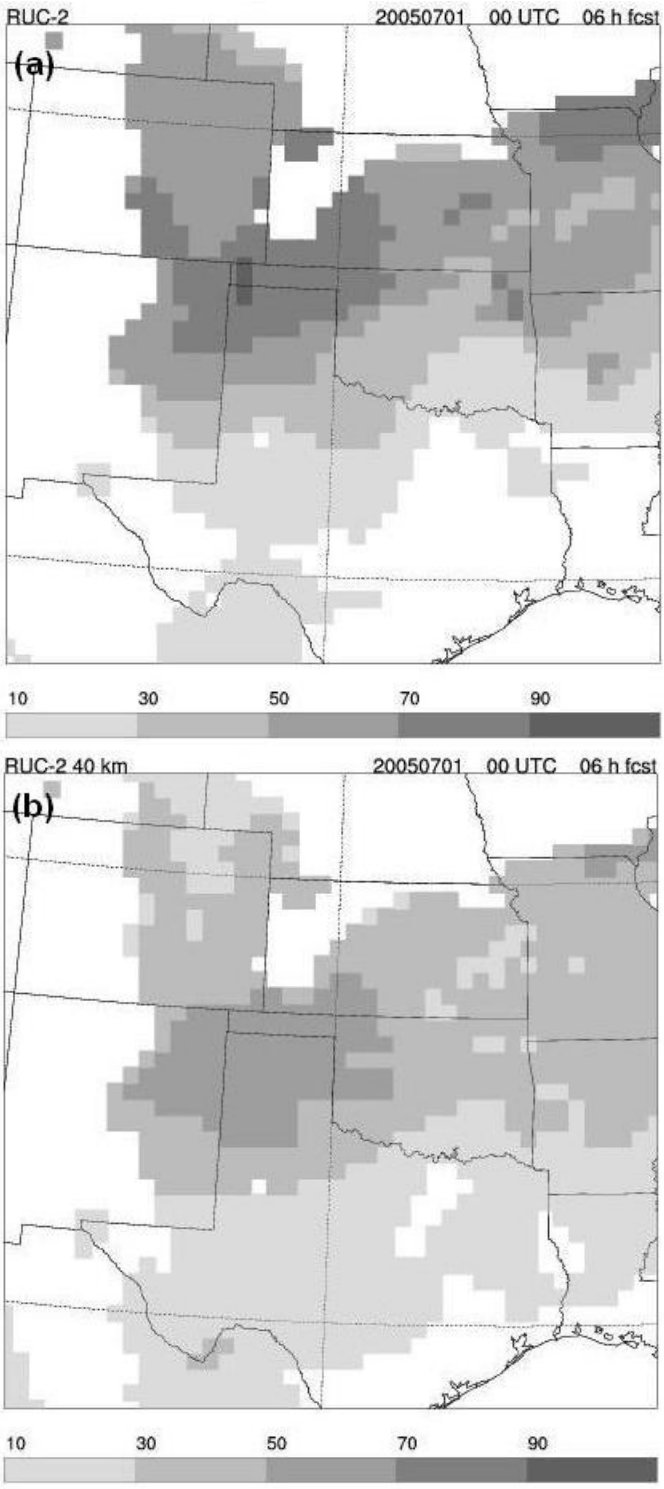

Fig. 12. (a) Values of the MCS maintenance probability (%) based on a 6-h RUC forecast valid at 0600 UTC 1 July 2005. (b) As in (a), except for the probability of MCS speed ≥ 18 m s^{-1}(%).